Article

Battery Model Identification Approach for Electric Forklift Application

Cynthia Thamires da Silva [1,*] , Bruno Martin de Alcântara Dias [1] , Rui Esteves Araújo [2,*] , Eduardo Lorenzetti Pellini [1] and Armando Antônio Maria Laganá [1]

1   PEA—Polytechnic School (POLI-USP), University of São Paulo, 05508-010 São Paulo, Brazil; alcantara.dias@usp.br (B.M.d.A.D.); elpellini@usp.br (E.L.P.); lagana@lsi.usp.br (A.A.M.L.)
2   INESC TEC, Faculty of Engineering, University of Porto, 4200-465 Porto, Portugal
*   Correspondence: cynthiathamires@usp.br (C.T.d.S.); raraujo@fe.up.pt (R.E.A.)

Abstract: Electric forklifts are extremely important for the world's logistics and industry. Lead acid batteries are the most common energy storage system for electric forklifts; however, to ensure more energy efficiency and less environmental pollution, they are starting to use lithium batteries. All lithium batteries need a battery management system (BMS) for safety, long life cycle and better efficiency. This system is capable to estimate the battery state of charge, state of health and state of function, but those cannot be measured directly and must be estimated indirectly using battery models. Consequently, accurate battery models are essential for implementation of advance BMS and enhance its accuracy. This work presents a comparison between four different models, four different types of optimizers algorithms and seven different experiment designs. The purpose is defining the best model, with the best optimizer, and the best experiment design for battery parameter estimation. This best model is intended for a state of charge estimation on a battery applied on an electric forklift. The nonlinear grey box model with the nonlinear least square method presented a better result for this purpose. This model was estimated with the best experiment design which was defined considering the fit to validation data, the parameter standard deviation and the output variance. With this approach, it was possible to reach more than 80% of fit in different validation data, a non-biased and little prediction error and a good one-step ahead result.

Keywords: battery models; battery management system; electric forklift; transfer function battery model; output error battery model; Hammerstein-Wiener battery model; nonlinear grey box battery model

1. Introduction

Batteries have been a key component for the electrification of different sectors in last decades. This is particularly true for batteries based on lithium-ion cells. Indeed, li-ion batteries (LIBs) have advantages in high energy density, long lifespan, lightweight design, and high efficiency [1–3]. Their applications range from energy type batteries of a few kWh in residential systems (smart homes) to MWh for the provision of grid ancillary services (smart grids) [4]. Because of that, understanding these batteries and improving their performance and safety are some of the keys to a sustainable world.

In this paper, we present a methodology for choosing the best battery model and the best experiment design for parameter identification with a focus on electric forklift application. Forklifts are part of the industrial environment and are critical resources that directly influence the overall efficiency of any manufacturing facility or warehouse [5,6]. Therefore, electric forklifts are widely used, and their improvement is certainly a main topic of research [5,7]. The energy savings during the lowering of the payload is discussed in [8,9], in which they could reach 56% of energy saving efficiency in one cycle. With these systems, it is possible to decrease the size of the battery pack or increase the battery lifetime. New

energy storage systems with lead acid battery and supercapacitor are discussed in [7,10]; in these systems, the battery is supported by the supercapacitors during high current request, increasing the battery lifetime. Systems with fuel cells are discussed in [11]; the authors concluded that is possible to work without interruptions with an electric forklift for 7 h 15 min. The sizing of a lithium-ion battery/supercapacitor hybrid energy storage system is discussed in [5], and a combination with fuel cell, lithium battery and supercapacitor is discussed in [12]. In [6], the authors compared the lead acid battery and the lithium battery applied in electric forklifts in an actual warehouse environment, evaluating the performance in terms of truck downtime, energy efficiency and truck productivity. Among other things, the authors concluded that the lithium-ion truck increased by 10% the number of pallets moved per operating hour. And from the total cost of ownership perspective, according to [13], the price of lithium batteries will decrease, and the total cost of ownership of electric forklifts with lithium batteries will decline.

A high-performance battery contributes to better energy efficiency and minimizes forklift downtime [6]. To ensure an efficient, reliable and safety battery operation, a battery management system (BMS) is required. The BMS has many tasks, but the most important one is battery state estimation. Accurate state estimation improves the battery autonomy, efficiency, safety and prolongs their lifespan. Some of these states are state of charge (SOC), state of health (SOH) and state of function (SOF). However, in practice, the battery state is a non-measurable variable, which can only be indirectly estimated through the continuous measurement of battery voltage, current and temperature. And due to the nonlinearities, accurate state estimation is a difficult task, and relies essentially, on proper battery model, good algorithms, and field tests [1]. This work aims to fulfil a gap in system identification procedures available in the literature for battery cells in order to include overall discussions, tests and statistical analysis on the proper models, best experiment design and optimizers. The proposed methodology was applied to electric forklift battery applications but can be easily suited to any other electrical mobility and battery storage scenarios.

1.1. Li-Ion Battery Model Main Issues

Recently, many battery models have been presented and studied. However, the pursuit for models with high accuracy and computational efficiency remains a challenge. There are many different battery models, and they can be classified in the following categories: equivalent circuit models (ECMs); electrochemical models; analytical and impedance-based models; and empirical and semiempirical models. All of them can predict battery performance, but with various levels of complexity and accuracy [2,14]. The differences between these models are presented in [15].

The battery is a complex electrochemical system which is both nonlinear and non-stationary. In other words, the relationship between the applied current and the output voltage is nonlinear [2]. In fact, the real world is nonlinear, and in some applications, these aspects cannot be ignored. Nonlinear models are instrumental in achieving a basic understanding of problems, in which researchers still struggle to comprehend for instance, when chemical reactions take place, affected by many other physical and electrical quantities and properties [14]. In addition, the battery is considered a nonstationary system because its internal electrical parameter characteristics change during a cycle of charge and discharge, as well as during its life cycle. Because of that, many researchers are working on the development of good and accurate descriptions of the li-ion battery behaviors, which consider three dominant variables: voltage, temperature, and aging [2].

Generating a mathematical model of a li-ion battery that can describe the input to output dynamics is a challenging problem [2,14], and deficiencies in the model structure (structural model errors) become quite common in the area. In any case, a model should be capable of producing a model output $y(t)$ based on previous input-output measurements and complying with practical experiments. These experiments must cover the domain of interest and bring out all essential system features needed [16]. Thus, the model must be chosen with focus on a final purpose. Depending on this purpose, it is possible to classify

battery models into short-term behavior models (which focus on SOC), long-term behavior models (which focus on SOH), and so on [14].

The model must also be chosen to describe the battery dynamic, and this dynamic can be totally different regarding application. For instance, a model that was developed to describe a residential energy storage system will be different from a model that describes the battery dynamic on a hybrid electric vehicle.

With a given data set and model set, an identification task is needed to select the model that best describes the observed data. Most estimation methods are based on a fit criterion between the observed output $y(t)$ and the model output $\hat{y}(t)$ [16].

Battery modelling is essential for safe charging and discharging, optimal battery utilization, fast charging and so on. One of the most important pieces of battery information—the battery range prediction—is only possible through advanced battery modelling and estimation techniques. Therefore, modelling plays an important role in the battery technology development and is vital for all applications [15].

1.2. Objectives and Contributions

The purpose of this paper is developing a model based on a battery ECM that will be used for state of charge estimation, in a battery applied in an electric forklift. To achieve this purpose, a system identification methodology presented in [17] is used, and four different types of battery models are tested and compared, from basic linear models to complex nonlinear schemes. All these models were previously used in other papers, achieving good results for their specific purposes. In this work, the main differences are highlighted, with additional information, so the future researchers and application engineers could choose the model that best fits with their purpose. Since the simplest model can somewhat describe a battery dynamic, the information provided in this paper can clarify most trade-offs between accuracy and complexity, which must be considered for practical application.

In addition, this paper presents and compares seven different experiment designs and their data sets. Focusing on an electric forklift application, the experiment type and the resulting data sets were tested against the models in order to select the best suited method that provides information for BMS algorithm evaluation and certification.

1.3. Paper Organization

Section 2 presents the battery modelling with the ECM and the state-space equations. This section also presents the OCV (open circuit voltage)—SOC nonlinear relationship and discusses different types of nonlinearity representation. Section 3 presents the system identification methodology, the studied battery cell characteristics, the experiment design, the methods for model validation, and a description of the most important models. Section 4 presents a comparison between those models, with the previously described validation methods. Section 4 also presents an analysis on the best experiment design for a model applied in state of charge estimation in electric forklift applications. At the end, a best model structure is presented, similar to the best optimizer and best experiment design. Section 5 presents the conclusions.

2. Battery Modelling

Equivalent circuit models are the most usual battery model, with the simplest structure and smallest computational load. These models are derived from empirical knowledge by applying idealized circuit elements such as resistance, capacitance, and voltage source to represent the electrical li-ion battery characteristics. There are different types of ECMs. The ECM selection is performed with a trade-off between good model accuracy and low computational complexity. A typical ECM generally uses resistors and capacitor branches to simulate the battery's dynamic characteristics. The more RC networks are used in the ECM, the higher would be the accuracy, as well the order and complexity [1,4].

An accurate battery model would require the representation of several physical phenomena, such as [4]:

- The OCV-SOC relationship
- The hysteresis effect
- Temperature
- Capacity rate impact
- Capacity degradation

Every feature added to the model will significantly increase the computational effort and the model complexity. Since complex models typically are more susceptible to uncertainties, models that are accurate enough and yet simple are preferred. In [18], a comparative study was performed with equivalent circuit models for li-ion batteries and concluded that the best representation for LiFePO4 is the first order RC model, with one state hysteresis (1RCH). Considering the study made in [18], in this paper, we develop a model with one RC branch considering the OCV-SOC relationship and the hysteresis effect. The model is represented in Figure 1.
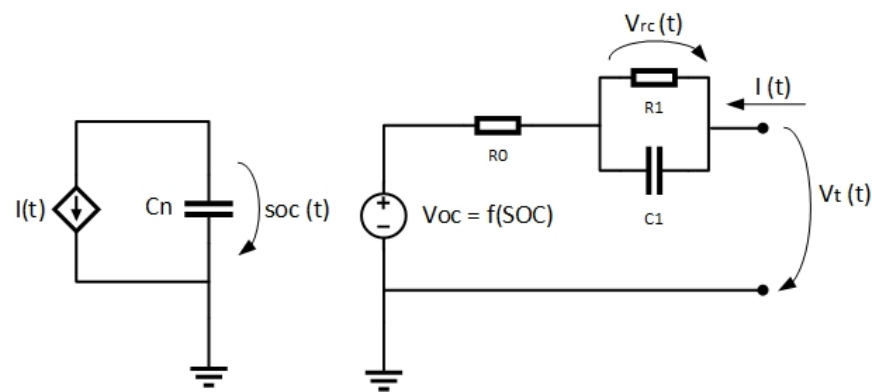

Figure 1. Equivalent circuit battery model.

Referring to the Figure 1 circuit, the voltage source is used to describe the SOC dependent OCV, R_0 is the battery ohmic resistance, and the RC parallel branch is a lumped analogy aimed to model polarization effects including, among others, charge, diffusion, convection, migration, and transfer effect on electrodes [19]. Considering Figure 1, the equations and states that represent this circuit are as follows: $u(t) = I(t)$; $y(t) = V_t(t)$; $x_1(t) = V_{RC}(t)$; $x_2(t) = soc(t)$. Where $u(t)$ is the input vector, $I(t)$ is the applied current vector, $y(t)$ is the output vector, $V_t(t)$ is the battery total voltage, $x_1(t)$ and $x_2(t)$ are the state vectors, $V_{RC}(t)$ is the voltage drop in the RC branch, and $soc(t)$ is the state of charge vector. The derivatives of the state's vectors are:

$$\dot{x}_1(t) = -\frac{1}{R_1 * C_1} * x_1(t) - \frac{1}{C_1} * u(t) \tag{1}$$

$$\dot{x}_2(t) = \frac{1}{3600 * Cn} * u(t) \tag{2}$$

where R_1 and C_1 are the battery equivalent circuit resistor and capacitor, and the Cn represents the battery nominal capacity.

$$y(t) = V_{OCV} - x_1(t) - R_0 * u(t) \tag{3}$$

One of the challenges of this type of model is to represent the nonlinear relationship between the OCV and SOC, represented in Equation (3) by the voltage V_{OCV}. There are many different forms to describe this relationship. The most common are:

- Lookup table
- Polynomial approximation
- Piecewise linear functions

For this work, all these methods were tested and, in general, the lookup table has good accuracy, despite its higher memory usage in the microcontroller used to implement the BMS functions. The polynomial approximation method is also a good option, with better accuracy and less memory consumption, but requires a seventh order polynomial, thus, a higher computation effort. However, this method is less accurate than a piecewise set of functions. The piecewise linear functions are easy to implement, have less computational requirements than high order polynomial approaches, and less memory footprint than the lookup table method. The piecewise functions adopted in this work employ 10 equally spaced intervals (breakpoints) from which the parameters b_0 (y-intercept) and b_1 (slope of the linear approximation) need to be previously calculated from the known OCV-SOC relationship. Ten equally spaced piecewise linear functions, similar to the ten breakpoints shown in Figure 2, have shown to be sufficient to properly describe the OCV-SOC behavior. The intermediate values in the curve can be found by means of simple interpolations.
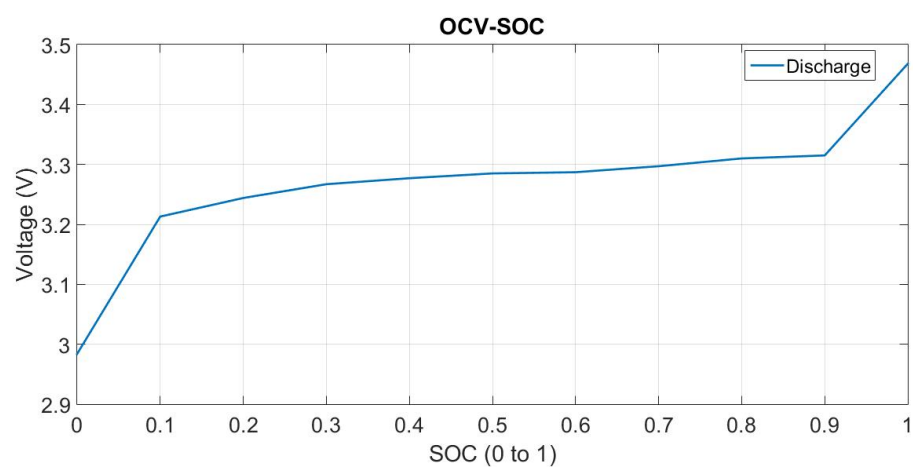
Figure 2. OCV-SOC breakpoints used in the model.

The results in each breakpoint for b_0 and b_1, are presented in Table 1.

Table 1. Parameter b_0 and b_1 in each SOC breakpoint.

SOC (%)	b_0	b_1	SOC (%)	b_0	b_1
10	2.9840	2.29	60	3.2750	0.02
20	3.1820	0.31	70	3.2270	0.1
30	3.1980	0.23	80	3.2060	0.13
40	3.2370	0.1	90	3.27	0.05
50	3.2450	0.08	100	1.938	1.53

Is important to mention that li-ion batteries have a hysteresis in the OCV-SOC relationship in charge and discharge modes. This typical cell hysteresis can be seen in Figure 3.
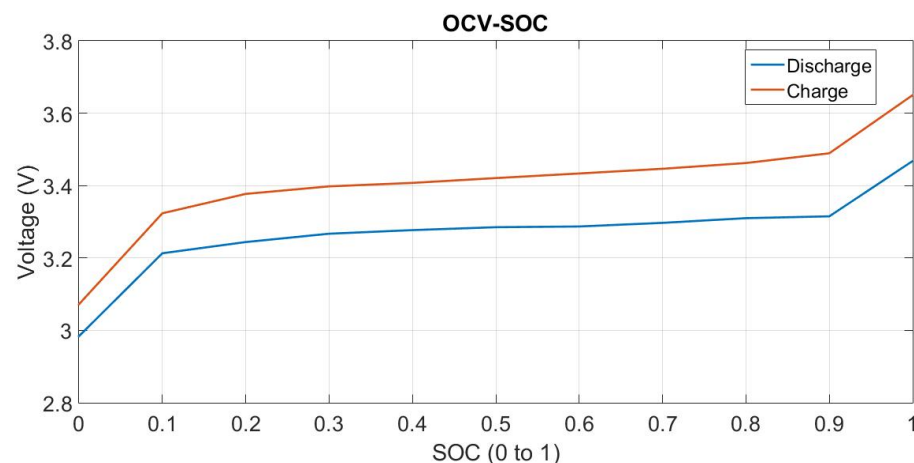
Figure 3. Battery cell hysteresis noticed in the OCV-SOC relationship.

The result presented in Figures 2 and 3 was achieved using the battery cell presented later in this article and the OCV test with 10 min of battery rest.

Since the OCV and SOC relationship is described by piecewise linear functions, each one represented by Equation (4), with different b_0 and b_1 values according with the *soc*:

$$V_{OCV} = b_0 + b_1 * soc \tag{4}$$

Replacing Equation (4) in Equation (3) results:

$$y(t) = -x_1(t) - R_0 * u(t) + b_0 + b_1 * soc \tag{5}$$

Considering Equation (5), the state-space equations that represent the battery's dynamics, can be written as follows:

$$\dot{x} = Ax + Bu \tag{6}$$

$$y = Cx + Du \tag{7}$$

$$\begin{bmatrix} \dot{x_1}(t) \\ \dot{x_2}(t) \end{bmatrix} = \begin{bmatrix} -\frac{1}{R_1 * C_1} & 0 \\ 0 & 0 \end{bmatrix} * \begin{bmatrix} x_1(t) \\ x_2(t) \end{bmatrix} + \begin{bmatrix} -\frac{1}{C_1} \\ \frac{1}{3600 * Cn} \end{bmatrix} * u(t) \tag{8}$$

$$y_1(t) = \begin{bmatrix} -1 & b_1 \end{bmatrix} * \begin{bmatrix} x_1(t) \\ x_2(t) \end{bmatrix} + [R_0] * u(t) + b_0 \tag{9}$$

where A is the state matrix, B is the input matrix, C is the output matrix, and D is the feedforward matrix.

In this model, R_0, R_1 and C_1 battery parameters should be identified. The C_n parameter is the battery nominal capacity, which can be found in the datasheet. The parameters b_0 and b_1 depend on the SOC, as shown before. It is important to notice that the ECM model accuracy relies on this model structure (its complexity in order and states) and on parameter identification accuracy.

3. Results

System identification is about building mathematical models of dynamic systems using measured input-output data [20]. Models are simplified representations of the real world, but still, they should provide an adequate representation of the underlying phenomena under study, which is the electric forklift in this paper. When properly created, they are a formidable tool to be used in complex analysis and decision situations [21]. Models may be delivered in various topologies and mathematical formalisms. The intended use will

determine the degree of sophistication that is required to make the model purposeful. The acceptance of a model should thus be guided by "usefulness" rather than "truth" [16,17].

According to [17], the construction of a model from observed data includes three basic entities, based in the researcher's previous knowledge and expertise:

- A data set—collected from an experiment, specially designed to expose relevant system behavior
- A set of candidate models—suited to represent the system dynamics
- An identification method—that tries to fit the model simulated results to the observed data set, adjusting the internal model parameters accordingly

In each one, simplifications are performed to describe, at first glance, the dominant states that rule the system behavior. However, since these states belong to a more complex nature, the decision about what is dominant or not may be proven wrong, mainly in systems where multi-domain interactions exist (i.e., electro-chemical, electro-thermal, electro-optics). This makes the system identification procedure to be a recursive and heuristic method, with several iterations, until the model passes all validation tests, which can assure its quality, for example, its capacity to reproduce the measured data [16,17].

In this paper, the following set of models, found in the literature, are studied as candidates for a battery cell representation, considering its open-circuit voltage and state of charge:

- Transfer function [22].
- Output error [23].
- Nonlinear Hammerstein-Wiener [24].
- Nonlinear Grey Box Model [25].

For parameter identification of ECM, the most popular approach is the least-squares method (LS). ECMs have multiple structure patterns and the mathematical equations of each model are different. According to [1], an optimizer may perform well for a certain set of problems but fail to address another set. Since the models have a nonlinear behavior, the least-squares method requires an iterative solution algorithm [22], with optimizers [26]. In this paper, the following set of candidate optimizers were compared:

- Subspace Gauss–Newton least squares and adaptive subspace Gauss–Newton [27].
- Levenberg–Marquardt least squares [28].
- Steepest descent least squares [29].
- Nonlinear least squares—trust region reflective [30].

So, with the model set and the optimizers algorithms defined, the first step according to the system identification loop described in [17] is the experiment design.

3.1. Experiment Design

In this paper, all the experiments were made with a battery cell, which is a LiFePO4 battery with 6 Ah of capacity. Table 2 shows the battery characteristics given by battery manufacturer.

Table 2. Battery cell characteristics.

Chemical	LiFePO4
Type	Cylindrical
Nominal capacity	6 Ah
Nominal voltage	3.2 V
Upper cut-off voltage	3.65 V
Lower cut-off voltage	2 V
Maximum continuous discharge current	1 C
Maximum continuous charge current	1 C

Many papers [21,31–40] used similar experiments designs to parameter estimation, considering fixed current pulses with the same characteristics presented in Figure 4. This type of test is quite common in OCV-SOC relationship estimation, as discussed in Section 2. However, in most papers, this type of experiment is used for parameter estimation in applications with different dynamic characteristics or they do not even specify the application, which makes the readers believe that this type of experiment design, will work for parameter estimation in any application. Following this line of thought, in this section we use the OCV test, with 10 min rest, for battery parameter identification. The input current and the output cell voltage of the complete OCV test are presented in Figure 4. However, the data set is especially important for battery modelling, and the best experiment design with focus on the application, in our case, the electric forklift, will be discussed in Section 4.1 and will be compared with this type of experiment.
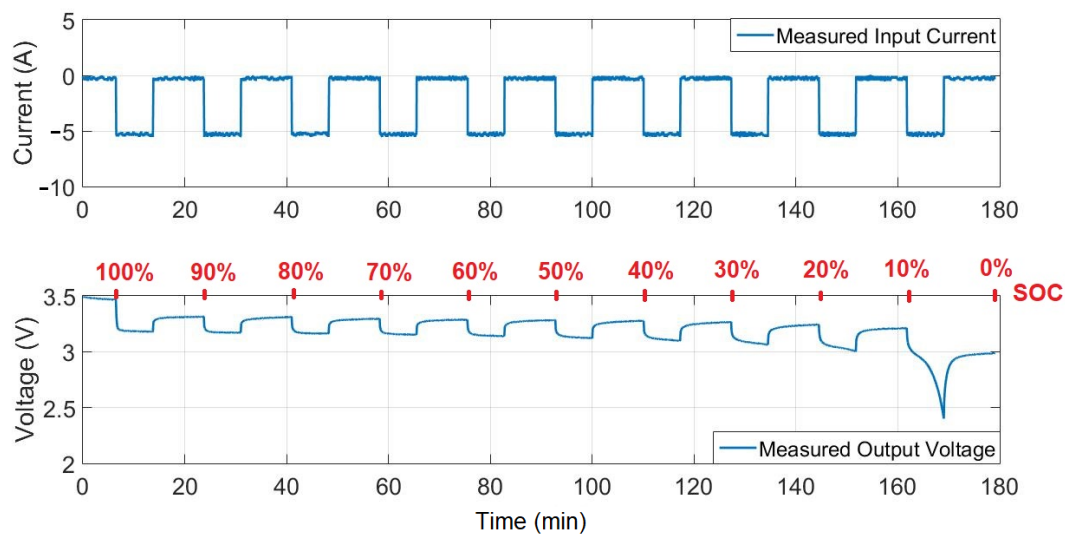

Figure 4. Complete OCV test measuring input current and output voltage.

To develop a good model, it is necessary to provide enough data for estimation and validation. According to [17], data must be different from each other. One way to provide enough data for a nonlinear system model estimation is to divide all the data into fraction parts and perform the estimation at different operating points of the system. This is because, if the data that explore all system non-linearity were used to perform estimation, the parameter's standard deviation will be higher.

According to [17], the estimation data must be 1/3 of the full system dynamics. Therefore, 1/3 of the test data were used for estimation and 1/3 for validation. As demonstrated in Figure 4, the battery used in this work has a similar dynamic between 90% and 30% of SOC. Therefore, for parameter estimation, data representing 80% to 50% of SOC were chosen because this fraction of data will be able to describe most of the battery dynamics. For model validation, data representing 50% to 20% of SOC were chosen. Therefore, the model will be validated with data that represent a different dynamic of the battery. In this case, models with good fit result in validation data (bigger nonlinearities) and will be even better in ranges of SOC with less nonlinearities. The estimation and validation data are presented in Figure 5.
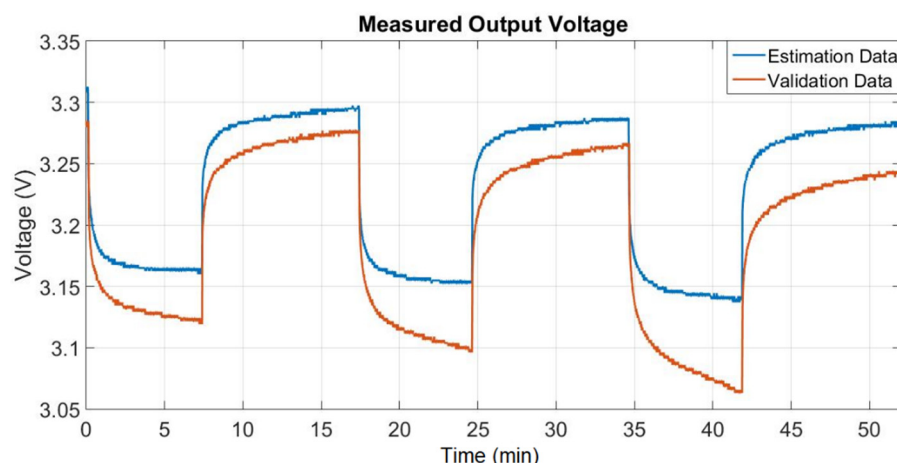
Figure 5. Estimation data (80% to 50% of SOC) and validation data (50% to 20% of SOC).

The measured output voltage and input current must be properly filtered because the measurement noises can affect the model parameter identification. Analyzing Figure 4, the measured output voltage is ready to use in the model estimation process; however, one may notice that the measured input current must be filtered, and its offset removed. So, a Butterworth low pass filter was employed. The developed filter was a second-order filter with easy digital implementation.

All experiment data were then properly selected and filtered from the designed experiments. However, we found interesting methods in the literature to compensate the noise-induced biases of model identification that can be applied in future works [19,41]. The following step is to study the model set with the input data.

3.2. Model Set

In these following sections, four different model structures are described and compared. The overall results are presented in Section 4.

3.2.1. Transfer Function

Considering a piecewise linear relationship between OCV-SOC, the battery model can be presented as a linear system transfer function with stepwise varying parameters. There are many papers that use transfer functions for battery modeling and [21] shows an interesting approach, where battery parameters can be extracted from the transfer functions coefficients. The transfer function developed in [21] is presented in Equation (10).

$$\frac{Y(s) - b_0}{U(s)} = \frac{\left(R_0 s^2 + \left(\frac{b_1}{C_n} + \frac{1}{C_1} + \frac{R_0}{R_1 * C_1}\right)s + \frac{b_1}{R_1 * C_1 * C_n}\right)}{s\left(s + \frac{1}{R_1 * C_1}\right)} \quad (10)$$

Using bilinear Z transform, a discrete transfer function, with sampling time T may be obtained:

$$\frac{\left(Y(z^{-1}) - b_0\right)}{U(z^{-1})} = \frac{c_0 + c_1 z^{-1} + c_2 z^{-2}}{1 + a_1 z^{-1} + a_2 z^{-2}} \quad (11)$$

where:

$$c_0 = \frac{T^2 b_1 + 2C_n R_0 T + 2C_n R_1 T + 4C_n R_0 R_1 C_1 + 2b_1 R_1 C_1 T}{2C_n T + 4C_n R_1 C_1}, \quad (12)$$

$$c1 = \frac{T^2 b_1 - 4C_n R_0 R_1 C_1}{C_n T + 2C_n R_1 C_1}, \quad (13)$$

$$c2 = \frac{T^2 b_1 - 2C_n R_0 T - 2C_n R_1 T + 4C_n R_0 R_1 C_1 - 2b_1 R_1 C_1 T}{2C_n T + 4C_n R_1 C_1}, \quad (14)$$

$$a_1 = \frac{-8C_n R_1 C_1}{2C_n T + 4C_n R_1 C_1}, \tag{15}$$

$$a_2 = \frac{-2C_n T + 4C_n R_1 C_1}{2C_n T + 4C_n R_1 C_1} \tag{16}$$

These equations were used for system identification, along with the following optimization methods: subspace Gauss-Newton least square, adaptative subspace Gauss-Newton, Levenberg-Marquardt least square, steepest descent least square and nonlinear least square. The best method for this transfer function model was the nonlinear least-square method. The result transfer function is presented in Equation (17).

$$\frac{\left(Y(z^{-1}) - 3.206\right)}{U(z^{-1})} = \frac{0.01317 - 0.02263z^{-1} + 0.00946z^{-2}}{1 - 1.82z^{-1} + 0.8203z^{-2}} \tag{17}$$

The battery parameters were then calculated using Equations (12)–(16) and the transfer function in Equation (17). The battery parameter results are: $b_1 = 2.2899$, $R_0 = 0.0119\ \Omega$, $R_1 = 0.0013\ \Omega$ and $C_1 = 3164.5$ F. With this approach, a 73.90% of fit was reached, as can be seen in Figure 6.
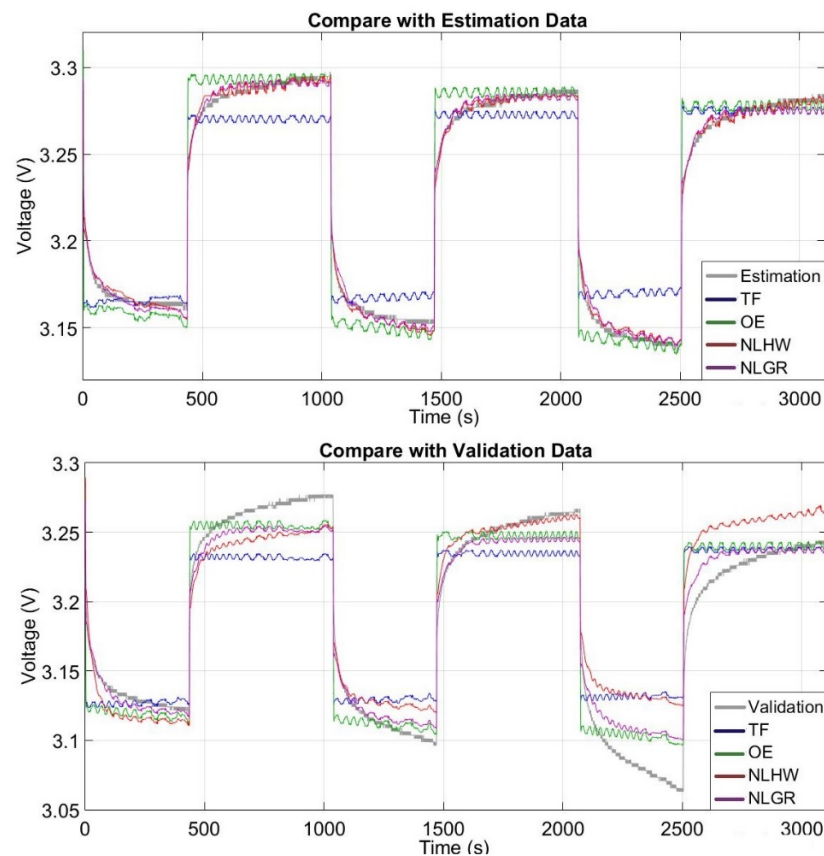
Figure 6. Comparison between each model response against estimation data and validation data.

3.2.2. Output Error Model

The output error models represent the discrete time transfer function that relates the measured current input to the measured battery voltage output, while also including white noise as an additive output disturbance. In [23], authors applied an interesting method using an output error model approach for battery parameter identification. In this work,

the transfer function previously developed in Section 3.2.1 was used, and the general output error model structure is presented in Equation (18).

$$y(t) = \frac{B(q)}{F(q)} u(t - n_k) + e(t) \tag{18}$$

where $y(t)$ s the output vector, $B(q)$ and $F(q)$ are the polynomial with respect to the backward shift operator z^{-1}, $u(t)$ is the input vector, n_k is the system delay and $e(t)$ is the system disturbance.

The orders of the output error model are:

$$nb : B(q) = b_1 + b_2 q^{-1} + \ldots + b_{nb} q^{-nb+1} \tag{19}$$

$$nf : F(q) = 1 + f_1 q^{-1} + \ldots + f_{nf} q^{-nf} \tag{20}$$

where nb and nf are the numerator and denominator order.

The estimative for the output error model through all optimization methods is presented in Table 4. According to this table, the nonlinear least-square method is the best optimization method for our output error model. The output error model is presented in Equations (21) and (22).

$$B(z) = 0.009828\,(\pm0.001447)z^{-1} - 0.01508(\pm0.003244)z^{-2} + 0.005254(\pm0.001834)z^{-3} \tag{21}$$

$$F(z) = 1 - 1.835(\pm0.02266)z^{-1} + 0.835(\pm0.02266)z^{-2} \tag{22}$$

The battery parameters were obtained using Equations (12)–(16), and the output error model in Equations (21) and (22). The battery parameter results are: $b_1 = 2.29$, $R_0 = 0.0115\ \Omega$, $R_1 = 0.0067\ \Omega$ and $C_1 = 3164.5$ F. With this approach, a 78.81% of fit was achieved, with results depicted in Figure 6.

3.2.3. Nonlinear Hammerstein-Wiener Model

In the Hammerstein-Wiener configuration, a linear system is placed between two different static nonlinear functions: a Hammerstein function located at input before the linear block, and a Wiener function placed right after, before the output. Adding these two functions improves the model flexibility and performance, as can be seen in [24], where authors use a Hammerstein-Wiener model for a battery system with an increase of 18% in the accuracy for the model when compared to a linear conventional transfer function model. In this work, the output error model presented in Section 3.2.2 was improved with the Hammerstein-Wiener approach, where the Wiener function is the relationship between OCV-SOC presented in Section 2. For this model, the best optimization method was the Levenberg–Marquardt least squares, which resulted in a fit of 93.94% between the estimation data and validation data. The results can be seen in Figure 6.

3.2.4. Nonlinear Grey Box Model

Grey box models combine prior physical knowledge with experimental data, for physical interpretation, to assign numerical values and range limits to model parameters. The grey box modeling technique emerged as a middle ground between white and black box models. In [25] a grey box model was developed for a battery and a supercapacitor, for accurate estimation of the SOC. In our work, the physical boundaries established for the grey box model parameters for the ECM are shown in Table 3.

Table 3. Battery system physical boundaries.

Parameter	Minimum Value	Maximum Value
R_0	0.001 Ω	0.1 Ω
R_1	0.001 Ω	0.5 Ω
C_1	100 F	50,000 F

In this type of model, we must inform initial states and parameters. The initial states were estimated through the nonlinear least-square trust-region reflective method, and the fit to the estimation data was 71%. The results for initial states, shown below, are valid since the estimation data starts with an SOC of 80%.

- $V_{RC} = 0.0573$ V
- SOC $= 84.77\%$.

The initial parameters were then calculated using the method presented in [31,42]. This method uses the OCV test presented in Figure 4, and the approach presented in Appendix A. The results for the initial parameters in 80% of SOC are:

- $R_0 = 0.0126$ Ω
- $R_1 = 0.0192$ Ω
- $C_1 = 8333.33$ F

Following Table 1, the initial parameter b_0 and b_1 in 80% of SOC are:

- $b_0 = 3.206$
- $b_1 = 0.13$

The best optimization method found for computation of the Nonlinear Grey Box model was the nonlinear least-squares trust-region reflective. The final battery parameters estimates are: $R_0 = 0.017241$ Ω, $R_1 = 0.00922729$ Ω, $C_1 = 3841.25$ F and the parameter b_1 was presented in Table 1. In this approach, a 93.13% of fit was achieved, as can be seen in Figure 6.

In this paper, four different optimizers algorithms, described in Appendix B, were compared, with results presented in Section 4. The model's results will be validated and compared using the fit result, the prediction error result, and the one-step ahead prediction, these methods are presented in Appendix C.

4. Comparing the Models

This section presents a comparison between the linear transfer function (TF), linear output error model (OE), nonlinear Hammerstein-Wiener model (NLHW), and nonlinear grey box model (NLGR). All these models were estimated trough the optimizers algorithm presented in Table 4. This table also presents the fit to estimation data in all models with all optimizers.

Table 4. Fit to estimation data with all optimization's methods in each model.

Optimization Method	Fit to Estimation Data			
	Transfer Function	Output Error	Hammerstein-Wiener	Nonlinear Grey Box Model
Subspace Gauss–Newton Least Square	68.76%	60.60%	79.58%	92.65%
Adaptative Subspace Gauss–Newton	54.64%	40.47%	93.80%	92.98%
Levenberg–Marquardt Least Square	70.13%	73.21%	93.94%	93.10%
Steepest Descent Least Square	−146.90%	−130.60%	24.56%	90.04%
Nonlinear Least Square	73.9%	78.34%	−234.10%	93.13%

A comparison between the fit result for each model is presented in Table 5, and the visual inspections can be made through Figure 6.

Table 5. Fit comparison between estimation data and validation data with TF, OE, NLHW, and NLGR.

Model	Fit to Estimation Data	Fit to Validation Data
TF	73.90%	58.73%
OE	78.81%	73%
NLHW	93.94%	63.01%
NLGR	93.13%	78.98%

Analyzing Table 5, the NLHW has a better fit result with the estimation data. But as discussed in Section 3.1, the parameter estimation must be made with one set of data, and the validation made with another set of data. In this case, using the validation data, the best result was achieved by the NLGR. This can be also noted through visual inspection of Figure 6.

Analyzing Figure 6, one can notice that the transfer function cannot represent the battery dynamic with good accuracy with both the estimation data and validation data. The model output voltage was not accurate, but the method presented in [21] is remarkably interesting. If the researcher's purpose is to use a simple approach, with low complexity but low accuracy, this could be a good choice.

The output error model with the parameter estimation method developed in [21] presents a better fit than the TF model. This makes sense since the output error structure includes white noise as an additive output disturbance. Therefore, the output error model describes the OCV-SOC nonlinear relationship better than transfer function. With the estimation data, this model response reaches the output battery voltage level, but still does not represent all battery dynamics behavior. Although, with the validation data, this model could not even achieve the output battery voltage level.

With the Hammerstein-Wiener model, where the OCV-SOC nonlinearity is represented by a function, the output result was incredibly good with the estimation data. The model can follow the output voltage level and the battery voltage dynamic. However, with the validation data, the model result could not reach all the output voltage levels. Comparing with previous model results, this model is a good option to represent the battery dynamics. This emphasizes the necessity to model nonlinearities within the model, for the fit result to be more accurate.

Finally, with the nonlinear grey box model, the results are remarkably close to the Hammerstein-Wiener result with estimation data. But with the validation data, this model presents the better result, among all others. This model fits satisfactorily in the nonlinear regions since some physical knowledge of the system is added in the process. This previous knowledge is capable to help the parameter identification methods to reach a good accuracy in the calculated values.

The estimated battery parameters with the best optimizers for each model are presented in Table 6.

Table 6. Estimated battery parameters in each model structure.

Battery Parameter	Transfer Function	Output Error	Hammerstein-Wiener	Nonlinear Grey Box Model
b_1	2.2899	2.29	Table 1	Table 1
$R_0(\Omega)$	0.0119	0.0115	0.0115	0.017241
$R_1(\Omega)$	0.0013	0.0067	0.0067	0.00922729
$C_1(F)$	3164.5	3164.5	3164.5	5841.25

We can see that the values of the parameters in the first three models are remarkably close. This totally makes sense, since these three models were developed in sequence, using the previous model structure from others. However, once the nonlinear grey box model uses a different approach, a little difference can be observed in the parameter values for this model. All these values are in the range that is specified in Table 3.

However, only with these values, a researcher cannot determine if the model is good or not. For this, the model will be validated with a prediction error method, which calculates the error between the output measured voltage and the output model voltage. The closer this result is to 0, the better is the model output accuracy. If this result is centered in 0, then the model may be called as non-biased. The prediction error method results are presented in Figure 7.
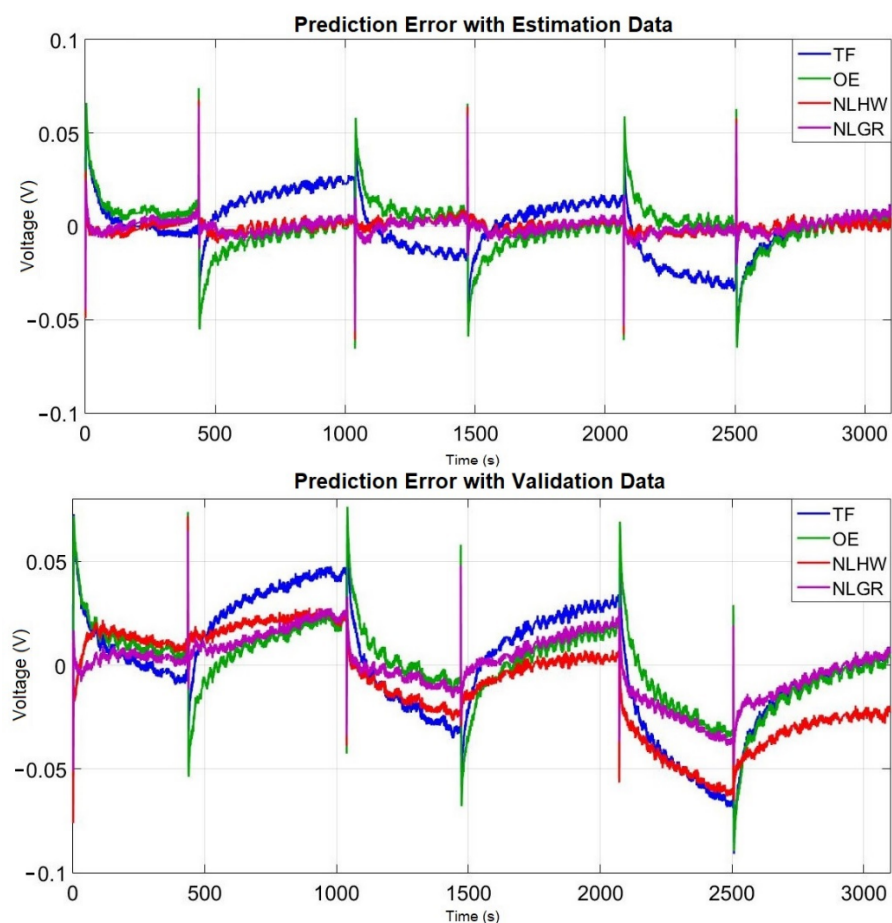
Figure 7. Prediction error with estimation data and validation data.

With the estimation data, the transfer function, and the output error present more output error than other methods. This happens because the two are linear models. However, the NLHW and the NLGR are non-biased since their results are close to 0. But with validation data, because of the battery nonlinearity in lower SOCs, the errors are bigger in all the models. This result shows the difficulty in all models to represent the battery output voltage in nonlinear regions. In this case, the NLHW present a result similar to the transfer function, and the bests results are the OE and the NLGR. This reassures the importance to validate the models with other methods besides a fit index related to estimation and validation data.

The purpose of this paper was to design a model to be used in SOC estimation. So, the model must be a prediction model, not a simulation one. Besides, an important validation to make is the one-step ahead prediction. This validation is presented in Figure 8.
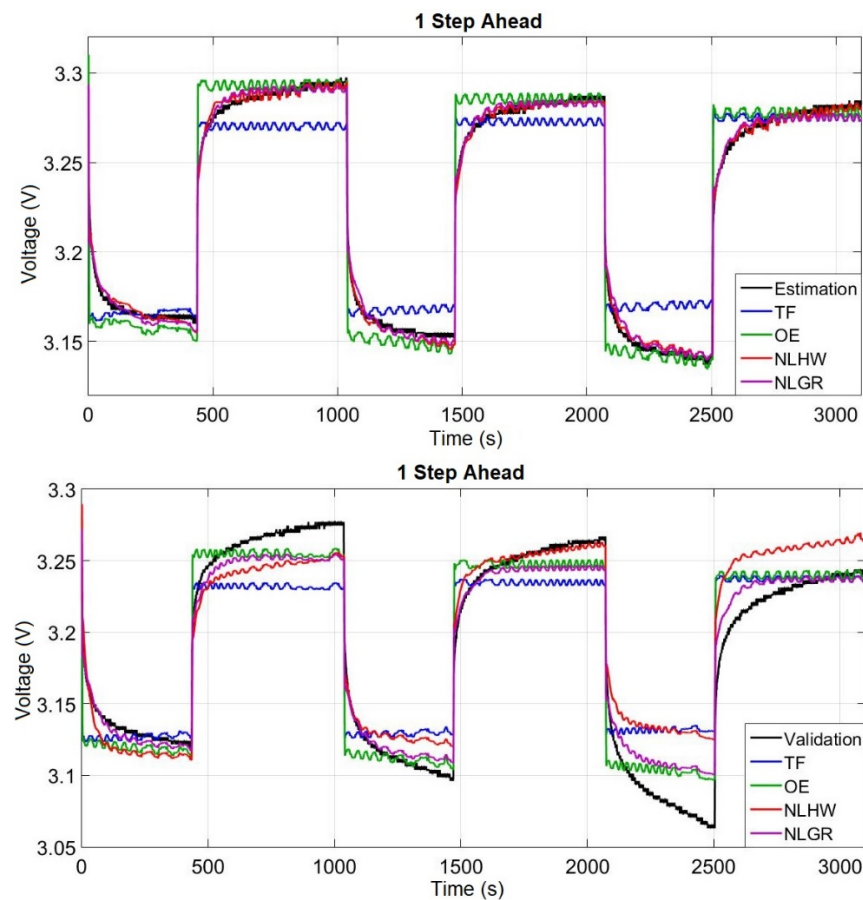
Figure 8. One-step ahead prediction with estimation data and validation data.

With the estimation data, only the NLHW and NLGR could predict the output battery voltage properly, with good accuracy. And with the validation data, all the models found difficulties to predict the battery output voltage in the nonlinear region. However, the NLGR model showed better results among others. Thus, the NLGR was selected as the best model for the forklift application. After choosing the model structure for our battery, according to [17], this model should also be validated with a data set that represents the battery dynamics for the forklift application.

4.1. Best Experiment Design

The previous estimations were made with the OCV test data, described in Section 3.1, and used in many papers [21,31–40]. However, this method is not appropriate to all applications, and the experiment design must be made with focus on the application [17]. The OCV test characteristics do not represent the precise forklift application energy dynamics and if the battery parameter estimation was made with this experiment, the model will not work properly [26], as presented in Table 7. So, a test was performed using an actual electric forklift, for 1 h, in a real scenario, using the same battery cell that was described earlier in this article. The electrical current measured in the electric forklift application, during its lifting and maneuvers, is presented in Figure 9.

Figure 9. Electric forklift battery application test.

From these measurements, experiment design was performed, with focus on the electric forklift's current dynamics. All tests were initiated with the battery totally charged, and the SOC was directly measured with a Coulomb counting algorithm. The experiment design set was divided into two groups:

- Group 1: long current pulses with 3 different resting times. The resting time is the moment when the forklift is near an idle state, where the current equals 0 A. These experiments are named "30 s of battery rest," "18 s of battery rest," and "5 s of battery rest." Figure 10 shows one of these experiments, with 5 s of resting time.
- Group 2: short current pulses with 2 different resting times and 2 different pulse periods, as presented in Figure 11. The pulses period is the moment when the current is different from 0 A, with a high variety of energy bursts. These experiments are named as "1 m high 30 s low," "30 s high 30 s low," and "30 s high 1 m low."

Figure 10. Long current pulses, with a resting time of 5 s during the bursts.
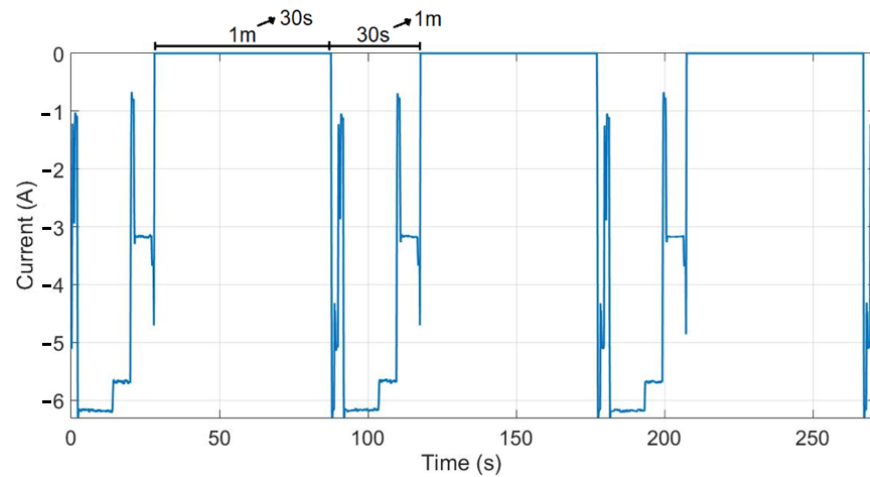
Figure 11. Short current pulses, where the currents are different from 0, with longer bursts.

The battery parameters in all these experiments used the Nonlinear Grey Box model previously presented in Section 3.2.4. The purpose here is to define the best experiment design for battery parameter estimation, that will be capable to be a better fit in the highest number of different experiment design. The various fit levels in all these experiments are presented in Table 7. In this table, the first column indicates the experiment that was used for estimation, and the other columns indicate the experiment used for validation.

Table 7. Comparison between all experiment data, regarding estimation data and validation data.

Estimation Data in 40% of SOC	Fit to Validation Data in 40% of SOC						
	30 s of Battery Rest	18 s of Battery Rest	5 s of Battery Rest	1 m HIGH 30 s LOW	30 s HIGH 30 s LOW	30 s HIGH 1 m LOW	OCV with 1 h of Rest
	V_{bat}	V_{bat}	V_{bat}	V_{bat}	V_{bat}	V_{bat}	V_{bat}
30 s of battery rest	93.09%	91.63%	84.75%	87.74%	84.04%	86.44%	37.49%
18 s of battery rest	91.37%	90.30%	86.16%	85.55%	82.03%	86.10%	54.31%
5 s of battery rest	84.36%	84.18%	83.52%	78.71%	76.34%	77.69%	49.38%
1 m HIGH **30 s** LOW	89.92%	89.28%	86.71%	90.57%	87.56%	90.06%	45.86%
30 s HIGH **30 s** LOW	83.70%	83.67%	85.69%	88.37%	89.56%	88.12%	43.41%
30 s HIGH **1 m** LOW	89.16%	88.32%	86.62%	90.03%	87.62%	90.47%	46.06%
OCV with **1 h** of rest	39.56%	32.03%	31.68%	52.79%	59.76%	59.64%	72.97%

All these estimations were made with 40% of SOC since, at this point, the battery dynamic has little nonlinearities and the fit to validation data will be more accurate. In Table 7 is possible to note that the best results appear when the estimation data and validation data are the same. These results are not considered because, as presented in [17], the model must be validated with a data set different from the one used for its estimation.

The estimations data that presents better fits to validation data are: "18 s of battery rest," "1 m high 30 s low" and "30 s high 1 m low". One important point to mention is the worst results. According to Table 7, the OCV test presents the worst results within all fit to validation data. This happens because the OCV test dynamic is hugely different from the

other experiments. This emphasizes that the battery models that were estimated with the OCV test, will not work properly on a battery applied in electric forklifts. However, the best experiment design should be defined considering other important information.

A proper way to check the estimated model accuracy with the best experiment design is the parameter standard deviation and the output variance [43,44]. A little value of the standard deviation shows that this parameter is important to explain the system dynamic when this model structure is chosen. And a little value in the output variance indicates that the model captures the estimation data in a good way [16,17]. The parameter standard deviation and the output variance are presented in Table 8.

Table 8. Estimated initial states, standard deviation, and output variance of all experiment designs.

Estimation Data in 40% of SOC	Standard Deviation			Output Variance
	R_0 (Ω)	R_1 (Ω)	C_1 (F)	V_{bat} (V)
30 s of battery rest	0.00784	0.00866	2783.49	0.002743
18 s of battery rest	0.008343	0.143	2979.6	0.003649
5 s of battery rest	0.009449	3.005	29,673	0.005321
1 m HIGH 30 s LOW	0.004475	0.005234	1488.38	0.004197
30 s HIGH 30 s LOW	0.00703	0.005927	1976.67	0.004973
30 s HIGH 1 m LOW	0.005395	0.006039	1752.36	0.004317
OCV with 1 h of rest	0.001426	0.001335	770.58	0.023996

The R_0 and R_1 standard deviation has little value in all experiments. These parameters are more important to explain the battery system with these experiment designs and this model structure. However, the C_1 standard deviation has a big value in all experiments. In Figure 12, it can be noted that the model result could not reach all the capacitance dynamics, thus resulting in a big C_1 standard deviation value.
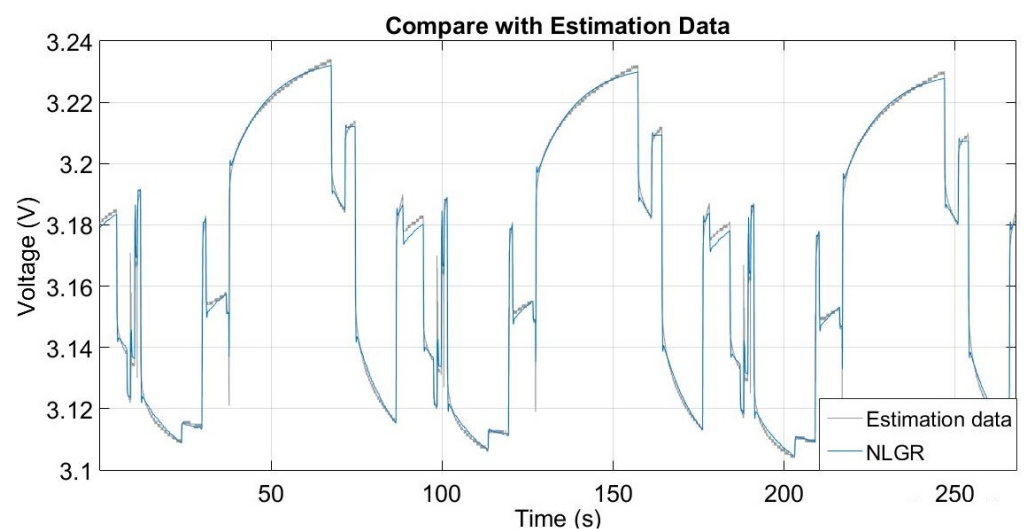

Figure 12. NLGR estimation data result with the best experiment design.

Among the experiments with the best fit results, the smallest standard deviation and smallest output variance are also marked in green. Therefore, the best experiment design for LiFePO4 batteries used in electric forklifts is the "1 m high 30 s low". As shown in Table 7, this experiment was able to identify the battery dynamic with good accuracy in different experiments characteristics ("5 s of battery rest" and "30 s high and 1 m low"), and as shown in Table 8, this experiment has a good accuracy in the estimated parameters

and estimated output. In other words, the identified parameters with this experiment are able to better describe the battery dynamics under different electric forklift use conditions.

It is important to mention that the best standard deviation result is presented in the "OCV with 1 h rest", however, this experiment has the worst output variance and fit to validation data results. This information shows the importance of evaluating more than one piece of information to choose the best experiment design for model estimation.

4.2. Nonlinear Grey Box Model Estimated with the Best Experiment Design

In this section, the nonlinear grey box model estimation is presented in more details. The following estimation will be made with the best experiment design presented in Section 4.1, with 40% of SOC. The initial states were estimated through the nonlinear least-squares optimization method. The fit to estimation data was 74.55% and the results are:

- $V_{RC} = 0.06703$ V
- SOC $= 29.17$ %.

As explained in Section 4.1, all the experiments were made with a parallel Coulomb counting algorithm, to provide another SOC measurement. In this case, the Coulomb counting SOC has a value of 40%, but the initial state estimation through the nonlinear least-squares optimization method results in 29.17%. This optimization method cannot achieve the correct value because the estimation data used cannot fully describe the state of charge. This is different from the OCV test used in Section 3.1, where the nonlinear least-squares optimization method achieved the correct value because in the OCV test the SOC are easy to determine. But with the best experiment design (1 m high 30 s low) the initial states estimation results prove that the algorithm was not capable to estimate the initial SOC accurately only with this portion of the experiment design. The initial parameters were calculated as described in Sections 2 and 3.2.4, but now, using the OCV with 1 h rest experiment. The nonlinear grey box model was estimated through nonlinear least squares, reaching a fit of 90.57%. This can be seen in Figure 12.

This figure depicts only the estimation data. The fit to each validation data can be seen in Table 7. As can be noticed in Figure 12, the estimation data and the output of the NLGR model have characteristics almost indistinguishable, which confirm that this model can represent the battery dynamics with good accuracy, even with different current pulses values and periods. These pulses characteristics are nearly the real one of the actual electric forklifts presented in Figure 9. The difference between the two curves can be noticed in Figure 13, which represents the prediction error with the estimation data.
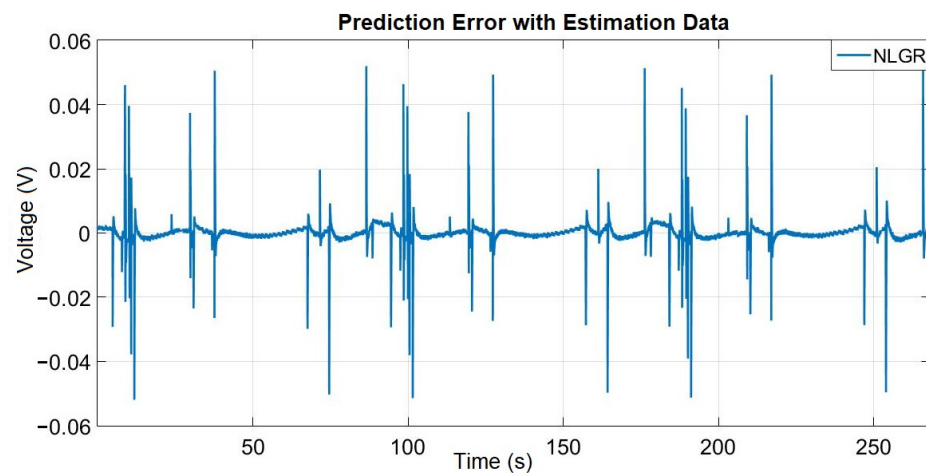

Figure 13. Prediction error validation with the best experiment design.

This result shows that the model is non-biased, and the error is always close to 0, which represents a good output model accuracy. The validation with 1 step ahead prediction is presented in Figure 14.
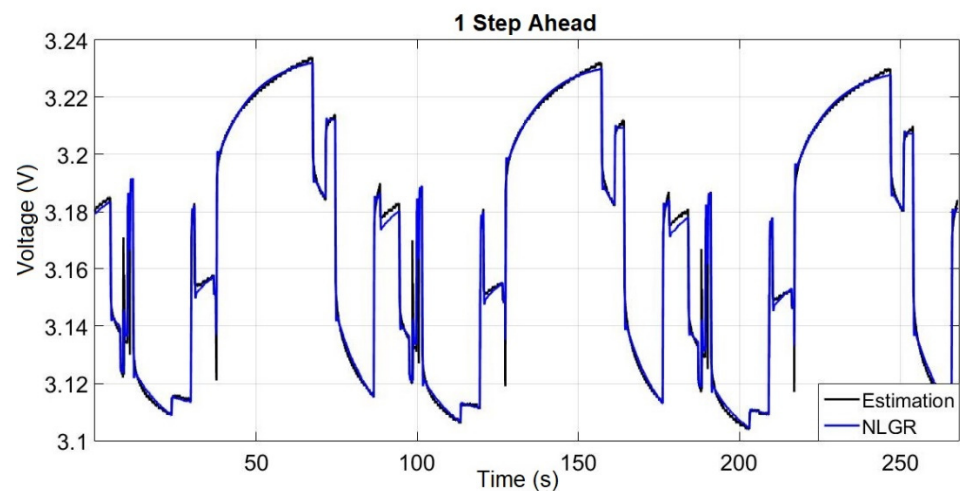
Figure 14. One-step ahead prediction with the best experiment design.

This model can predict the output with one-step ahead with good accuracy. Therefore, the nonlinear grey box model was properly validated with all methods and can be used for battery SOC estimation on this electric forklift application.

Now, making the identification procedure with this experiment design, in all points of SOC, we have the parameters presented in Table 9.

Table 9. Battery parameters in all points of SOC.

SOC (%)	b_0	b_1	R_0 (Ω)	R_1 (Ω)	C_1 (F)
10	2.8710	3.35	0.0140197	0.027101	420.558
20	3.1670	0.39	0.013602	0.012339	833.847
30	3.1810	0.32	0.0133872	0.00998571	1109.31
40	3.253	0.08	0.0132749	0.009014	1249.35
50	3.281	0.01	0.013237	0.00825815	1399.3
60	3.266	0.04	0.0131549	0.00771709	1473.69
70	3.152	0.23	0.0131347	0.00740307	1526.64
80	3.25	0.09	0.0132971	0.00777491	1509.14
90	3.314	0.01	0.0135692	0.00822862	1445.43
100	2.126	1.33	0.0153566	0.0072376	1927.32

These parameters are the nonlinear grey box model estimation results using the experiment "1 m high 30 s low", which was designed with a focus on the electric forklift battery dynamic, presented in Figure 9, and were chosen between other six different experiments presented in Table 7. The validation of the NLGR model result was performed by comparing the measured battery voltage and the model battery voltage as presented in Figure 12, which reaches 90.57% of accuracy with an error of no more than 50 mV as presented in Figure 13.

The parameters presented in Table 9 are important to describe with good accuracy a battery dynamic in an electric forklift application and is necessary information for a good battery SOC estimation algorithm applied in a BMS to use in a real electric forklift operation.

5. Conclusions

In this paper, the best battery model, with the best optimizer method and the best experiment design for a battery applied on an electric forklift was developed. With the

approach presented here, we develop a good model for our purpose, comparing four different models with four different optimizers and validating with the methods proposed by [17] with different experiment designs. The best experiment design was defined comparing the results with seven different experiments, each one designed based on the electric forklift scenario. The experiments have different input current amplitudes and periods, representing different types of the electric forklift usage.

As demonstrated in this work, the nonlinear grey box model is more accurate regarding the fit to validation data, with 78.98% of accuracy, comparing the measured output voltage and the model output voltage, also have less prediction error than the other methods with no more than 55 mV and can predict the battery output voltage with 1 step ahead better than the other models. The best optimizer for this model was the least-squares trust region method, which achieves 93.13% of fit and has little computational effort. The best experiment design was the experiment with 1 min of current pulses and 30 s of battery rest and was defined with focus on the battery electric forklift dynamic. With this experiment, it was possible to represent different levels of the battery dynamics, and the model estimated with this experiment was capable to fit with more than 86% in most validation data sets. Furthermore, this experiment presents a good parameter standard deviation, with 4.4 mΩ in the R_0 parameter, 5.2 mΩ in the R_1 parameter and 1488 F in the C_1 parameter. The big C_1 standard deviation happens because the model result could not reach all the capacitance dynamics with this experiment design, but this happens in all experiments made in this paper because the battery electric forklift dynamic does not reach all the battery capacitance dynamics. The chosen experiment design also has only 4.1 mV in the output variance.

As future work, it is intended to develop a model capable of providing sufficient data for initial states accurate estimation for the nonlinear grey box model in any experiment design. Further, it is also planned to implement a battery SOC estimation (with the model approach developed in this paper) to be used on actual electric forklift BMS.

Author Contributions: Conceptualization, R.E.A., E.L.P. and C.T.d.S.; methodology, C.T.d.S., R.E.A. and E.L.P.; software, B.M.d.A.D.; validation, R.E.A., E.L.P. and A.A.M.L.; formal analysis, E.L.P. and R.E.A.; investigation, C.T.d.S. and B.M.d.A.D.; resources, R.E.A., E.L.P. and A.A.M.L.; data curation, B.M.d.A.D.; writing—original draft preparation, C.T.d.S.; writing—review and editing, E.L.P. and R.E.A.; visualization, B.M.d.A.D.; supervision, R.E.A. and E.L.P.; project administration, A.A.M.L.; funding acquisition, A.A.M.L. All authors have read and agreed to the published version of the manuscript.

Conflicts of Interest: The authors declare no conflict of interest.

Nomenclature

Symbol	
BMS	Battery Management System
B(q), B(z)	Polynomial with respect to the backward shift operator z^{-1}
b_0	y-intercept parameter
b_1	parameter slope of the linear approximation
C_1	Battery Equivalent Circuit Capacitor
C_n	Battery nominal capacity
ECM	Equivalent Circuit Models
EV	Electric Vehicle
F(q), F(z)	Polynomial with respect to the backward shift operator z^{-1}

HEV	Hybrid Electric Vehicle
LIB	Li-Ion Battery
LiFePO4	Lithium Iron Phosphate Battery
LS	Least Square method
nb, nf	Numerator and denominator order
NLGR	Nonlinear Grey Box model
NLHW	Nonlinear Hammerstein Wiener model
n_k	System delay
OCV	Open Circuit Voltage
OE	Output Error
PHEV	Plug-in Hybrid Electric Vehicle
R_0, R_1	Battery Equivalent Circuit Resistors
RC	Resistor/Capacitor circuit
RCH	Resistor/Capacitor circuit with one State Hysteresis
SOC	State of Charge
SOF	State of Function
SOH	State of Health
TF	Transfer Function
V_{OCV}	Nonlinear relationship between the OCV and SOC
V_{bat}	Battery total voltage (V)
Vector and Matrix	
A	State matrix
B	Input matrix
C	Output matrix
D	Feedforward matrix
e(t)	System disturbance
I(t)	Applied current vector (A)
soc(t)	State of charge vector
u(t)	Input vector
$V_{RC}(t)$	Voltage drop in Resistor/Capacitor circuit
$V_t(t)$	Battery total voltage (V)
$x_1(t), x_2(t)$	State vectors
$\dot{x}_1(t), \dot{x}_2(t)$	State vector derivative
$y(t), \hat{y}(t)$	Output vector

Appendix A. Initial Battery Parameters Calculation

In this case, the initial state was 80% of SOC, so, only the portion of the OCV test that represents 80% of SOC was selected. This portion is presented in Figure A1.
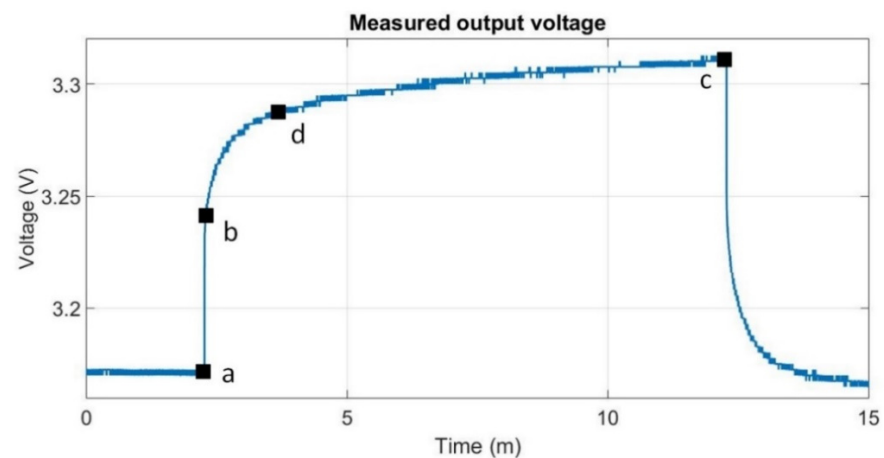

Figure A1. Measured points to calculate parameters R_0, R_1 and C_1 at 80% of SOC.

According to the points presented in Figure A1, the following equations were applied to determine the parameters.

$$R_0 = \frac{b - a}{I} \tag{A1}$$

where a is the exact point that current drops and voltage rises, b. is the subsequent point where other dynamics take place, and I is the current applied during the OCV test.

$$R_1 = \frac{c - b}{I} \tag{A2}$$

where c is the exact point that current was again applied.

$$d = ((c - b) * 0.633) + b \tag{A3}$$

$$t_b - t_d = T \tag{A4}$$

where t_b is the time instant for point b, t_d is the time instant for point d, and T is the C_1 time constant.

$$C_1 = \frac{T}{R_1} \tag{A5}$$

Appendix B. Criterion of Fit

In this paper four different optimizers algorithm, described in the following sections, were compared.

Appendix B.1. Gauss-Newton Method

The Gauss-Newton method is a well-known iterative technique used regularly for solving the nonlinear least squares problem. The Gauss-Newton method consists in solving a sequence of linearized least squares approximations to the nonlinear problem, each of which can be solved efficiently by an 'inner' direct or iterative process. In comparison with Newton's method and its variants, the Gauss-Newton method for solving the nonlinear least squares problem is attractive because it does not require computation or estimation of the second derivatives of the function and hence is numerically more efficient [45]. The Gauss-Newton method is a method for minimizing a sum-of-squares objective function. It presumes that the objective function is approximately quadratic in the parameters near the optimal solution. For moderately sized problems the Gauss-Newton method typically converges much faster than gradient-descent methods [26]. In the field of battery modelling, in [27], they use the Gauss-Newton method for lithium-ion battery parameter identification.

Appendix B.2. Levenberg-Marquardt Algorithm

The Levenberg–Marquardt algorithm combines two numerical minimization algorithms: Gauss–Newton method and gradient descent method. In the Gauss–Newton method, the sum of the squared errors is reduced by assuming the least square function is locally quadratic in the parameters and finding the minimum of this quadratic. In the gradient descent method, updating the parameters in the steepest-descent direction the sum of the squared errors is reduced. The Levenberg–Marquardt method acts more similar to the Gauss–Newton method when the parameters are close to their optimal value and acts more akin to a gradient-descent method when the parameters are far from their optimal value [26]. The Levenberg–Marquardt algorithm is based on a trust region reflective similar principal. By a factor that is calculated from one step to another, the iteration step size is increased. This provides a robust algorithm, despite having poor start parameters in the direction of the steepest descent. It combines the advantages of Gauss–Newton method and steepest descent method [28]. In [28], the battery parameter identification is made using the Levenberg–Marquardt algorithm.

Appendix B.3. Steepest Descent Method

The steepest descent method is a general minimization method which updates parameter values in the "downhill" direction: the direction opposite to the gradient of the objective function [26]. In [29] they used the steepest descent method, among other methods for curve-fit the baseline battery system.

Appendix B.4. Trust-Region Method

In the trust-region expansion, the iteration increment is increased. In the confidence interval, a defined radius around the iterate, the algorithm searches for a greater minimum as it is defined by the normal increment. This allows the process to converge extremely fast toward the steepest descent [28]. Within a small subset, the trust region method searches for the optimal solution. This subset can be approximated around the initial position using a model function. Because the battery model parameters are usually limited within a range, the trust region reflective method can be used to bound the model parameters by applying a single reflection transformation. By nature, trust region reflective is a local exploitation method, making its performance heavily affected by initial points [30]. In [30] they use the trust-region method to parameterize battery models.

Appendix C. Model Validation

In identification and optimization process, the model parameters are more accurate when the model battery voltage are closer to the measured battery voltage [1]. One of the most common and pragmatic tools for model validation is cross validation, which checks how well the model can reproduce the behavior of new data sets (validation data) that were not used to estimate the model. One way is producing a simulated model output $\hat{y}(t)$ using the validation data input and compare how well this model output reproduces the validation data output $y(t)$. The comparison could simply be a subjective, ocular inspection of the plots to see if essential aspects of the system for the intended application are adequately reproduced [16,17].

The comparison can also be done by computing numerical measures of the fit between the two signals. These are naturally based on the distance between $y(t)$ and $\hat{y}(t)$. A common numerical measure is the *fit*, presented in Equation (A6).

$$fit = 100 \left(1 - \frac{\sqrt{\| \sum y(t) - \hat{y}_s(t) \|^2}}{\sqrt{\| \sum y(t) - mean(y(t)) \|^2}} \right) \text{ (in \%)} \tag{A6}$$

The fit determines the percentage of how much of the output variation is correctly reproduced by the model [16,17]. In other words, the model battery voltage and the measured battery voltage can be employed as the best value that fits to access the model parameters and acquire the optimal model parameters that make the model battery voltage closest to the measured battery voltage [1].

Other important method for models that contain integration or are used for control design, which is our case, is the evaluation of the model's prediction capability. The k-step-ahead predicted output for validation data $\hat{y}_p(t|t-1)$. It means that $\hat{y}_p(t|t-1)$ is the $y(t)$ model's prediction, based on all relevant past inputs and all outputs up to time $t-k$. The prediction can then be compared with the measured validation output by inspecting the plots or by the fit criterion presented in Equation (A6) [16,17].

References

1. Lai, X.; Gao, W.; Zheng, Y.; Ouyang, M.; Li, J.; Han, X.; Zhou, L. A Comparative Study of Global Optimization Methods for Parameter Identification of Different Equivalent Circuit Models for Li-Ion Batteries. *J. Electrochim. Acta* **2019**, *295*, 1057–1066. [CrossRef]
2. Mesbahi, T.; Rizoug, N.; Bartholome, P.; Sadoun, R.; Khenfri, F.; Moigne, P. Dynamic Model of Li-Ion Batteries Incorporating Electrothermal and Ageing Aspects for Electric Vehicle Applications. *IEEE Trans. Ind. Electron.* **2018**, *65*, 1298–1305. [CrossRef]
3. Tran, N.; Khan, A.B.; Nguyen, T.; Kim, D.; Choi, W. SOC Estimation of Multiple Lithium-Ion Battery Cells in a Module Using a Nonlinear State Observer and Online Parameter Estimation. *Energies* **2018**, *11*, 1620. [CrossRef]
4. Misyris, G.S.; Papadopoulos, T.A.; Agelidis, V.G. State of Charge Estimation for Li-Ion Batteries: A More Accurate Hybrid Approach. *IEEE Trans. Energy Convers.* **2019**, *34*, 109–119. [CrossRef]
5. Paul, T.; Mesbahi, T.; Durand, S.; Flieller, D.; Uhring, W. Sizing of Lithium-Ion Battery/Supercapacitor Hybrid Energy Storage System for Forklift Vehicle. *Energies* **2020**, *13*, 4518. [CrossRef]
6. Alshaebi, A.; Dauod, H.; Weiss, J.; Yoon, S.W. Evaluation of Different Forklift Battery Systems Using Statistical Analysis and Discrete Event Simulation. In Proceedings of the 2017 Industrial and Systems Engineering Conference, Pittsburgh, PA, USA, 20–23 May 2017.
7. Dezza, F.C.; Musolino, V.; Piegari, L.; Rizzo, R. Hybrid Battery-Supercapacitor System for Full Electric Forklifts. *IET Electr. Syst. Transp.* **2019**, *9*, 16–23. [CrossRef]
8. Minav, T.A.; Murashko, K.; Laurila, L.; Pyrhonen, J. Forklift with a Lithium-Titanate Battery during a Lifting/Lowering Cycle: Analysis of the Recuperation Capability. *Autom. Constr.* **2013**, *35*, 275–284. [CrossRef]
9. Yu, Y.X.; Ahn, K.K. Energy Saving of an Electric Forklift with Hydraulic Accumulator. In Proceedings of the 2019 19th International Conference on Control, Automation and Systems (ICCAS), Jeju, Korea, 15–18 October 2019; pp. 408–411. [CrossRef]
10. Conte, M.; Genovese, A.; Ortenzi, F.; Vellucci, F. Hybrid Battery-Supercapacitor Storage for an Electric Forklift: A Life-Cycle Cost Assessment. *J. Appl. Electrochem.* **2014**, *44*, 523–532. [CrossRef]
11. Lototskyy, M.V.; Tolj, I.; Parsons, A.; Smith, F.; Sita, C.; Linkov, V. Performance of Electric Forklift with Low-Temperature Polymer Exchange Membrane Fuel Cell Power Module and Metal Hydride Hydrogen Storage Extension Tank. *J. Power Sources* **2016**, *316*, 239–250. [CrossRef]
12. Hsieh, C.; Nguyen, X.; Weng, F.; Kuo, T.; Huang, Z.; Su, A. Design and Performance Evaluation of a PEM Fuel Cell—Lithium Battery—Supercapacitor Hybrid Power Source for Electric Forklifts. *Int. J. Electrochem. Sci.* **2016**, *11*, 10449–10461. [CrossRef]
13. Jiao, M.; Pan, F.; Huang, X.; Yuan, X. Evaluation on Total Cost of Ownership of Electric Forklifts with Lithium-Ion Battery. In Proceedings of the 2021 IEEE 4th International Electrical and Energy Conference (CIEEC), Wuhan, China, 28–30 May 2021; pp. 1–5. [CrossRef]
14. Relan, R.; Firouz, Y.; Timmermans, J.; Schoukens, J. Data Driven Nonlinear Identification of Li-Ion Battery Based on a Frequency Domain Nonparametric Analysis. *IEEE Trans. Control Syst. Technol.* **2017**, *25*, 1825–1832. [CrossRef]
15. Fotouhi, A.; Auger, D.J.; Propp, K.; Longo, S.; Wild, M. A Review on Electric Vehicle Battery Modelling: From Lithium-ion toward Lithium-Sulphur. *J. Renew. Sustain. Energy Rev.* **2016**, *56*, 1008–1021. [CrossRef]
16. Schoukens, J.; Ljung, L. Nonlinear System Identification—A User Oriented Road Map. *IEEE Control Syst. Mag.* **2019**, *39*, 28–99. [CrossRef]
17. Ljung, L. *System Identification. Theory for the User*, 2nd ed.; Prentice Hall: Hoboken, NJ, USA, 1999; ISBN 0-13-656695-2.
18. Hu, X.; Li, S.; Peng, H. A Comparative Study of Equivalent Circuit Models for Li-Ion Batteries. *J. Power Sources* **2012**, *198*, 359–367. [CrossRef]
19. Wei, Z.; He, H.; Pou, J.; Tsui, K.; Quan, Z.; Li, Y. Signal-Disturbance Interfacing Elimination for Unbiased Model Parameter Identification of Lithium-Ion Battery. *IEEE Trans. Ind. Inform.* **2020**, *17*, 5887–5897. [CrossRef]
20. Ljung, L. Prediction Error Estimation Methods. *Circuits Syst. Signal Process.* **2002**, *21*, 11–21. [CrossRef]
21. Bradley, S.P.; Hax, A.C.; Thomas, L.M. *Applied Mathematical Programming*, 5st ed.; Addison Wesley Publishing Company: Boston, MA, USA, 1977; ISBN 020100464X.
22. Rahimi-Eichi, H.; Baronti, F.; Chow, M.Y. Modeling and Online Parameter Identification of Li-Polymer Battery Cells for SOC Estimation. In Proceedings of the IEEE International Symposium on Industrial Electronics, Hangzhou, China, 28–31 May 2012. [CrossRef]
23. Ma, Y.; Zhou, X.; Li, B.; Chen, H. Fractional Modeling and SOC Estimation of Lithium-ion Battery. *J. Autom. Sin.* **2016**, *3*, 281–287. [CrossRef]
24. Firouz, Y.; Mierlo, V.J.; Bossche, P.V. Nonlinear Modeling of all Solid-State Battery Technology based on Hammerstein Wiener Systems. In Proceedings of the IEEE Electrical Power and Energy Conference, Montreal, QC, Canada, 16–18 October 2019. [CrossRef]
25. Navid, Q.; Hassan, A. An Accurate and Precise Grey Box Model of a Low-Power Lithium-Ion Battery and Capacitor/Supercapacitor for Accurate Estimation of State of Charge. *Batteries* **2019**, *5*, 50. [CrossRef]
26. Gavin, H. *The Levenberg-Marquardt Algorithm for Nonlinear Least Squares Curve-Fitting Problems*; Department of Civil and Environmental Engineering, Duke University: Durham, NC, USA, 2020. Available online: http://people.duke.edu/~{}hpgavin/ce281/lm.pdf (accessed on 24 February 2021).

27. Lass, O.; Volkwein, S. Parameter Identification for Nonlinear Elliptic-Parabolic Systems with Application in Lithium-Ion Battery Modeling. *Comput. Optim. Appl.* **2015**, *62*, 217–239. [CrossRef]

28. Westerhoff, U.; Kurbach, K.; Lienesch, F.; Kurrat, M. Analysis of a Lithium-Ion Battery Model Based on Electrochemical Impedance Spectroscopy. *Energy Technol.* **2016**, *4*, 1620–1630. [CrossRef]

29. Henson, W. Optimal Battery/Ultracapacitor Storage Combination. *J. Power Sources* **2008**, *179*, 417–423. [CrossRef]

30. Xie, F.; Yu, H.; Long, Q.; Zeng, W.; Lu, N. Battery Model Parameterization Using Manufacturer Datasheet and Field Measurement for Real-Time HIL Applications. *IEEE Trans. Smart Grid.* **2020**, *11*, 2396–2406. [CrossRef]

31. Liao, C.; Li, H.; Wang, L. A Dynamic Equivalent Circuit Model of LiFePO4 Cathod Material for Lithium-Ion Batteries on Hybrid Electric Vehicles. In Proceedings of the IEEE Vehicle Power and Propulsion Conference, Dearborn, MI, USA, 7–10 September 2009. [CrossRef]

32. Adu-Sharkh, S.; Doerffel, D. Rapid Test and Non-Linear Model Characterization of Solid-State Lithium-Ion Batteries. *J. Power Sources* **2004**, *130*, 266–274. [CrossRef]

33. Chen, M.; Rincon-Mora, G.A. Accurate Electrical Battery Model Capable of Predicting Runtime and IV Performance. *IEEE Trans. Energy Convers.* **2006**, *21*, 504–511. [CrossRef]

34. He, H.; Xiong, R.; Fan, J. Evaluation of Lithium-Ion Battery Equivalent Circuit Models for State of Charge Estimation by an Experimental Approach. *Energies* **2011**, *4*, 582–598. [CrossRef]

35. He, H.; Xiong, R.; Guo, H. Online Estimation of Model Parameters and State of Charge of LiFePO4 Batteries in Electric Vehicles. *Appl. Energy* **2012**, *89*, 413–420. [CrossRef]

36. Huria, T.; Ceraolo, M.; Gazzarri, J.; Jackey, R. High Fidelity Electrical Model with Thermal Dependence for Characterization and Simulation of High-Power Lithium Battery Cells. In Proceedings of the IEEE International Electric Vehicle Conference, Greenville, SC, USA, 4–8 March 2012. [CrossRef]

37. Rahmoun, A.; Biechl, H. Parameters Identification of Equivalent Circuit Diagrams for Li-Ion Batteries. In Proceedings of the 2012 11th International Symposium, Pärnu, Estonia, 16–21 January 2012.

38. Gallo, D.; Landi, C.; Luiso, M.; Morello, R. Optimization of Experimental Model Parameter Identification for Energy Storage Systems. *Energies* **2013**, *6*, 4572–4590. [CrossRef]

39. Rahimi-Eichi, H.; Baronti, F.; Chow, M. Online Adaptive Parameter Identification and State of Charge Coestimation for Lithium-Polymer Battery Cells. *IEEE Trans. Ind. Electron.* **2014**, *61*, 2053–2061. [CrossRef]

40. Santos, S.R.; Marques, F.L.R.; Nascimento, T.C.; Beck, R. A Brief Overview of Battery Management Systems for Lithium-Ion Batteries: Modeling, Estimation and Control. In Proceedings of the 10th Seminar on Power Electronics and Control, Santa Maria, Brazil, October 2018.

41. Wei, Z.; Dong, G.; Zhang, X.; Pou, J.; Quan, Z.; He, H. Noise-Immune Model Identification and State-of-Charge Estimation for Lithium-Ion Battery Using Bilinear Parameterization. *IEEE Trans. Ind. Electron.* **2021**, *68*, 312–323. [CrossRef]

42. Matos, M.R.S. Study and Parameter Estimation of an Electric Battery Model. Master's Thesis, Department of Electrical and Computer Engineering, University of Porto, Porto, Portugal, January 2010.

43. Rice, J.A. *Mathematical Statistics and Data Analysis*, 3rd ed.; Thomson Higher Education: Belmont, CA, USA, 2007; ISBN 978-8131519547.

44. Johnson, R.A.; Wichern, D.W. *Applied Multivariate Statistical Analysis*, 6th ed.; Prentice Hall: Hoboken, NJ, USA, 2007; ISBN 978-0-13-187715-3.

45. Gratton, S.; Lawless, A.S.; Nichols, N.K. Approximate Gauss-Newton Methods for Nonlinear Least Squares Problems. *SIAM J. Optim.* **2007**, *18*, 106–132. [CrossRef]